Compression behaviour of nanostructured NANOPERM alloy at 500 °C

V. D. COJOCARU[a,*], R. NICULA[b], M. STIR[b], E. BURKEL[b]
[a]*Politehnica University of Bucharest, Spl. Independentei 313, 060042 Bucharest, Romania*
[b]*University of Rostock, Physics Department, August-Bebel-Str. 55, D-18055, Rostock, Germany*

Over the last two decades, nanocrystalline materials were investigated for applications in magnetic devices. The benefits of nanocrystalline alloys stem from their chemical and structural variations over nanometer scale which are important for developing optimal magnetic properties. Over the last decade less attention has been paid to the stability of nanostructured materials under extreme conditions of pressure and temperature. The main aim of the present work is to study the behaviour of soft magnetic nanostructured $Fe_{88}Zr_7B_4Cu_1$ (NANOPERM) alloy under high pressure – high temperature conditions. The αFe (bcc) crystalline cell at 500^0C for pressures up to 3.5 GPa was evaluated using synchrotron radiation X-ray diffraction.

(Received August 23, 2011; accepted October 20, 2011)

Keywords: Magnetic materials, Nanostructured materials, Crystalline cell compression

1. Introduction

Amorphous and nanocrystalline materials were recently investigated for applications in magnetic devices such as transformers, inductive devices, etc, which use soft-magnetic materials [1]. The interest in developing nanocrystalline soft-magnetic alloys has dramatically increased during the past few years. Bulk soft-magnetic materials need to have both high induction and permeability, as well as many other non-magnetic features such as mechanical properties, corrosion resistance, etc [2].

Nanocrystalline soft magnetic alloys can be described in general as $TL_{(1-x)}(TE, M, NM)_x$, where TL denotes a late (ferromagnetic) transition metal element, TE denote an early transition metal element , M is a metalloid, and NM is a noble metal. This composition usually has $x < 0.20$ i.e. with as much late ferromagnetic transition metals (TL = Co, Ni or Fe) as possible. The early transition metals (TE = Zr, Nb, Hf, Ta, etc.) and metalloids (M = B, P, Si, etc.) are added to promote glass formation in the precursors. The noble metal elements (NM = Cu, Ag, Au, etc.) serve as nucleating agents for the ferromagnetic nanocrystalline phase [1, 3-7].

Nanocrystalline alloys incorporating α-Fe nanocrystalline phases are being explored as alternative soft magnetic materials with improved properties. Excellent soft magnetic properties result due to a fine distribution of crystalline grains within an amorphous matrix [2-7].

NANOPERM-type alloys are based on the Fe-TM-B system; they contain larger concentrations of Fe (83-89 at.%) and have higher values of saturation induction (~ 1.6 – 1.7 Tesla). The NANOPERM nanocrystalline alloys have very low energy losses at power frequencies (60 Hz), making them potentially interesting for electrical power distribution transformers [1].

Over the last decade high induction bulk materials, including NANOPERM-type alloys, were investigated, however less attention has been paid to the stability of nanostructured materials under extreme conditions of pressure and temperature [8]. It is known that high pressure has a great impact upon phase transition, at high values for applied pressure metastable structures can be obtained, which can lead to new possible application for such materials.

The aim of present study is to investigate the behaviour of αFe (bcc) crystalline cell under extreme conditions of pressure and temperature.

2. Experimental

Nanocrystalline powder precursors for the NANOPERM-type soft magnetic alloy $Fe_{88}Zr_7B_4Cu_1$ were obtained by high-energy ball-milling (Retsch 400 PM planetary ball-mill) starting from high-purity elemental powders with an average particle-size close to 250 μm. The elemental powders were immersed in hexane and mechanically milled in stainless steel vials (250 ml) with stainless steel balls (20 mm diameter) at 250 rpm. The ball-to-powder mass ratio was 20:1 and the total milling time was 90 hours [9]. The obtained NANOPERM powders were subject to morphological investigation using a scanning electron microscope TESCAN VEGA II – XMU.

The αFe (bcc) crystalline cell behaviour under extreme conditions of pressure and temperature was investigated in compression experiments performed at F2.1 beamline instrument from DESY/HASYLAB

(Hamburg, Germany). The pressure-temperature region under investigation was restricted to pressure values of up to 4 GPa for a temperature of 500 °C. The experiments were performed in EDX (Energy Dispersion X-Ray Diffraction) mode.

Fig. 1 show schematic representation of used diffractometer, the scanning was performed in EDX mode with 2θ fix angle. The NANOPERM powders were embedded in a sample holder, which can be hydrostatically compressed at a desired pressure level.

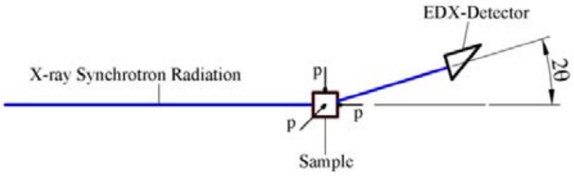

Fig. 1. Schematic representation of measurement method.

Fig. 2 shows the sample holder construction scheme. The desired temperature program is achieved by Joule effect, DC current is applied to the upper and lower part of the sample holder, DC current is passing through the upper graphite disc – graphite cylinder – lower graphite disc, resulting heat. The temperature is recorded using a thermocouple. Inside the graphite cylinder the NANOPERM powder is embedded in a boron nitride layer which ensures sample isolation. In the upper part of the sample holder a layer of NaCl is necessary in order to determine the value of applied hydrostatic pressure.

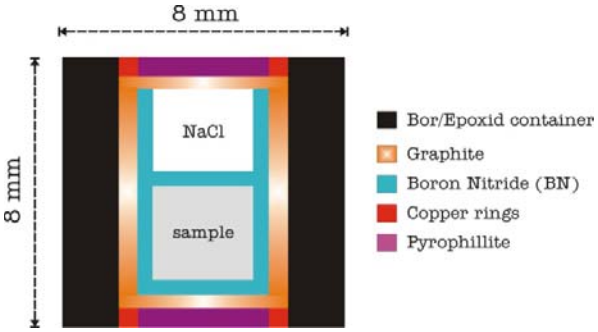

Fig. 2. Sample holder construction scheme.

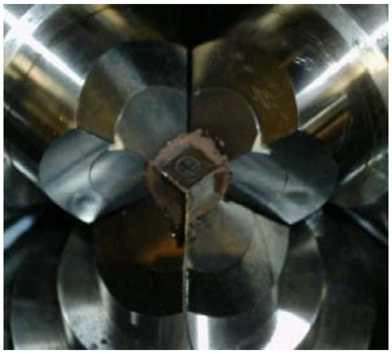

Fig. 3. Relative position of anvils and sample holder.

The hydrostatic pressure is applied by 6 anvils, the position of anvils and sample holder is showed in Fig. 3.

Once the pressure is applied, the press can be moved on vertical scale, ensuring the pass of the X-ray beam trough the sample holder. To determine the value of applied pressure, the X-ray beam must pass through the NaCl layer. The recorded variation in NaCl (110) peak position gives input information for NaCl Decker's equation of state and the real value of applied pressure in the sample holder can be calculated. After determination of applied pressure value, the press is moved on vertical scale to ensure the pass of X-ray beam through NANOPERM powder and its XRD spectra being recorded.

3. Results and discussion

3.1 NANOPERM powders morphology

In Fig. 4 SEM images of NANOPERM powders obtained after 90 hours of ball-milling are presented at different magnifications. As observed in Fig. 4, one can see that the resulted powders show a placketar (flakes-like) layered morphology (see Fig. 4-a) and an uniform distribution in size, due to the high intensity particle fragmentation at higher ball-milling times, the average particle size being situated close to approx. 9 μm (see Fig. 4-b). A small fraction of particles with small dimensions (bellow 2 μm) are present onto larger particles.

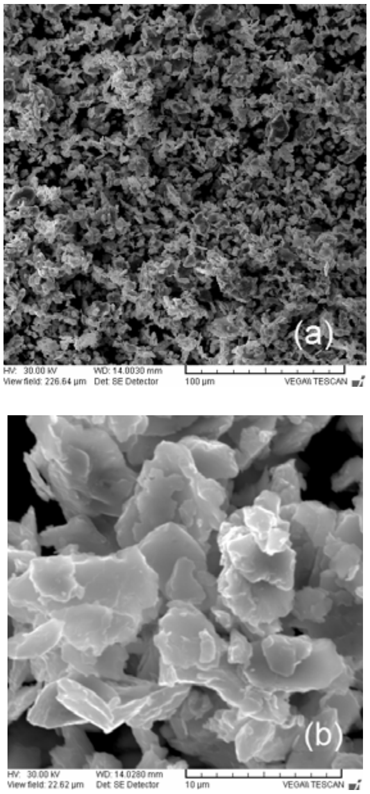

Fig. 4. SEM images for NANOPERM powders ball-milled for 90 h, at different magnifications.

3.2. Compression behaviour of NANOPERM powders

In order to determine the value of applied pressure the recorded peaks of NaCl were acquired at desired temperatures and pressure levels (see Fig. 5). One can observe that applying temperature (see Fig. 5-b) the (200)NaCl peak shift to lower energy values, due to the thermal expansion of the crystalline cell. Applying pressure shift the (200)NaCl peak to higher energy values due to de crystalline cell compression (see Fig. 5-c).

In order to determine the applied pressure Decker's equation of state for NaCl was used [10], knowing the d-spacing (interplanar distance) and applied temperature the resulted applied pressure can be easily calculated.

The d-spacing parameter can be easily calculated at different temperature and pressure levels using a linear relation, such as:

$$E_{NaCl\ d(200)}\ x\ d_{200} = E'_{NaCl\ d'(200)}\ x\ d'_{200} \tag{1}$$

where $E_{NaCl\ d(200)}$ is the energy of (200)NaCl peak, d_{200} is the d-spacing of (200)NaCl peak, $E'_{NaCl\ d(200)}$ is the energy of (200)NaCl peak at applied temperature and d'_{200} is the d-spacing of (200)NaCl peak at applied temperature.

The $E_{NaCl\ d(200)}\ x\ d_{200}$ represents an experiment constant and give easy solution to determine the d'_{200}:

$$d'_{200} = \frac{E_{NaCl\ d(200)}\ x\ d_{200}}{E'_{NaCl\ d'(200)}} \tag{2}$$

A similar equation can be used in order to determine the d-spacing in the case of applied temperature and pressure:

$$E_{NaCl\ d(200)}\ x\ d_{200} = E''_{NaCl\ d(200)}\ x\ d''_{200} \tag{3}$$

where $E''_{NaCl\ d(200)}$ is the energy of (200)NaCl peak at applied temperature and pressure and d''_{200} is the d-spacing of (200)NaCl peak at applied temperature and pressure.

Same formalism can be applied in the case of (110), (200) and (211) bcc-αFe peaks, such as:

$$E_{NaCl\ d(200)}\ x\ d_{200} = E_{Fe\ d(110)}\ x\ d_{110} \tag{4}$$

$$d_{110} = \frac{E_{NaCl\ d(200)}\ x\ d_{200}}{E_{Fe\ d(110)}} \tag{5}$$

In same way de d-spacing for (200) and (211) bcc-αFe peaks can be calculated.

Compression experiments were carried out at applied pressures up to 3.5 GPa (see Table 1). In Fig. 6 a recorded X-ray diffraction pattern at p = 1.262 GPa and t = 500°C, is presented. One can observe the (110), (200) and (211) peaks of the bcc-αFe phase and also BN peaks coming from sample holder. The obtained diffraction patterns were fitted using the Peakfit v4.11 software package (Systat Software Inc.) and NANOPERM bcc-αFe (110), (200) and (211) peaks were substracted.

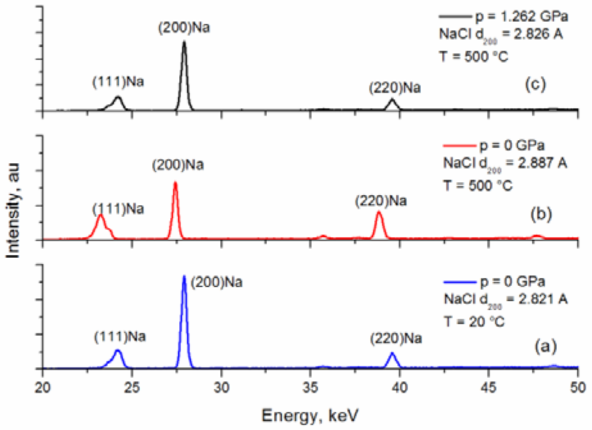

Fig. 5. Diffraction pattern of NaCl at different temperatures and applied pressures.

Table 1. Applied pressures.

Experiment no.	Applied pressure, GPa	Applied temperature, °C
1	0.329	500
2	0.831	500
3	1.072	500
4	1.262	500
5	1.582	500
6	1.956	500
7	2.333	500
8	2.556	500
9	2.807	500
10	2.864	500
11	3.012	500
12	3.408	500
13	3.475	500

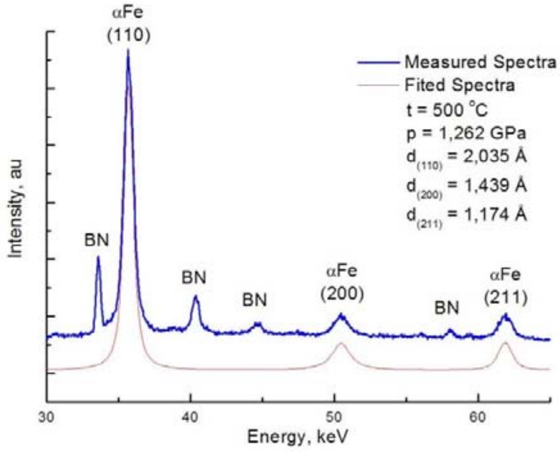

Fig. 6. Diffraction pattern of NANOPERM powders at p = 1.262 GPa and t = 500°C.

Variations of applied pressure induce changes in bcc-αFe diffraction peaks position, these changes shows the changes in NANOPERM crystalline cell. The refining of crystalline cell was performed using the ERACEL software package. Data concerning interplanar distances $d_{(110)}$; $d_{(200)}$ and $d_{(211)}$ at different applied pressure values was obtained.

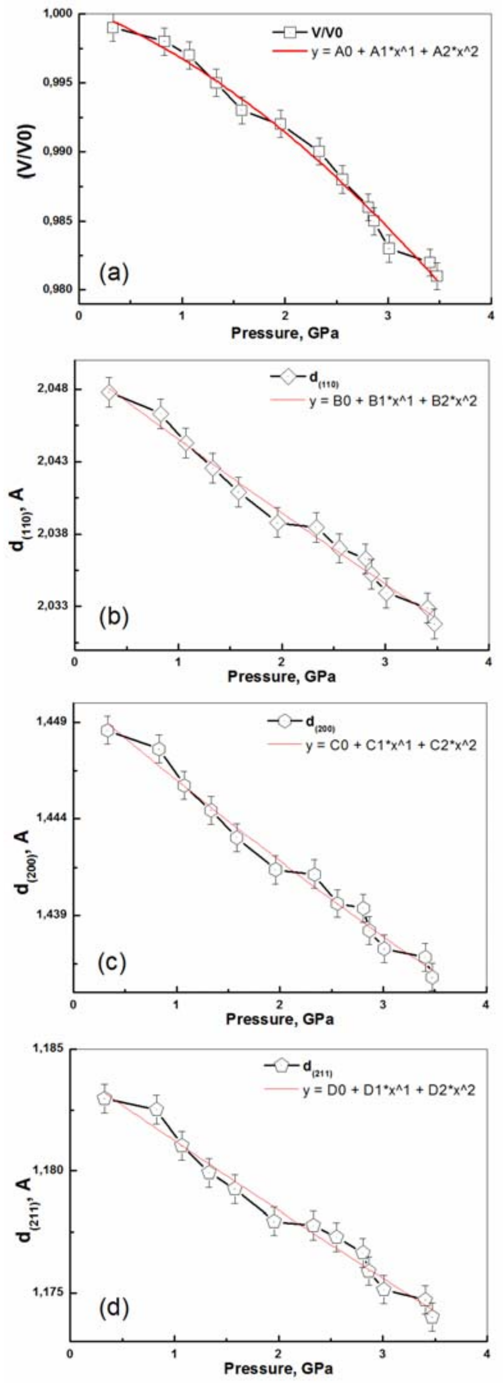

Fig. 6. Pressure influence upon crystalline cell volume (a) and interplanar distances $d_{(110)}$ (b); $d_{(200)}$ (c) and $d_{(211)}$ (d).

In Fig. 7 are presented the obtained data concerning applied pressure influence upon crystalline cell volume (see Fig. 7-a) and interplanar distances (d-spacing) $d_{(110)}$ (see Fig. 7-b); $d_{(200)}$ (see Fig. 7-c) and $d_{(211)}$ (see Fig. 7-d). One can observe that the crystalline cell volume decreases with increasing of applied pressure, the maximum of variation (V/V_0) is reached for an applied pressure of approx. 3.5 GPa when the compression of the crystalline cell is approx. 1.9%. The interplanar distances $d_{(110)}$; $d_{(200)}$ and $d_{(211)}$ exhibit a similar behaviour, decreasing with increasing the applied pressure. The variation laws of applied pressure influence upon crystalline cell volume and interplanar distances $d_{(110)}$; $d_{(200)}$ and $d_{(211)}$ can be approximated with a fair degree of accuracy using order one or two polynomial functions. Work is in progress to simulate and quantitatively describe the variation laws of applied pressure influence.

4. Conclusions

The compressibility of the bcc α-Fe structure was evaluated using synchrotron radiation X-ray diffraction, main conclusions resulting from experimental data processing are:

- at 500 °C in the pressure range up to 3.5 GPa, the $d_{(111)}$, $d_{(200)}$ and $d_{(211)}$ values decrease with increasing the applied pressure;
- the (V/V_0) crystalline cell volume variation is shifted to lower values with increasing pressure, for an applied pressure of 3.5 GPa, the pressure gradient determine a decreasing of (V/V_0) parameter with approx. 1,9 %;
- obtained results can be fitted with a very good accuracy using order one or two polynomial functions.

Work is in progress to simulate and quantitatively describe the variation laws of applied pressure influence.

References

[1] M. E. McHenry, M. A. Willard, D. E. Laughlin, Prog. Mater. Sci. **44**, 291 (1999).
[2] M. E. McHenry, M. A. Willard, H. Iwanabe, R. A. Sutton, Z. Turgut, A. Hsiao, D. E. Laughlin, Bull. Mater. Sci. **22**, 495 (1999).
[3] I. Skorvanek, J. Marcin, T. Krenicky, J. Kovac, P. Svec, D. Janickovic, J. Magn. Magn. Mater. **304**, 203 (2006).
[4] M. Kowalczyk, J. Ferenc, X. B. Liang, T. Kulik, J. Magn. Magn. Mater. **304**, e651 (2006).
[5] W. Lu, B. Yan, R. Tang, J. Alloys Compd. **425**, 406 (2006).
[6] J. S. Blazquez, C. F. Conde, A. Conde, S. Roth, A. Guth, J. Magn. Magn. Mater. **304**, e627 (2006).
[7] W. Lu, L. Yang, B. Yan, W. Huang, B. Lu, J. Alloys Compd. **413**, 85 (2006).
[8] M. Maglierini, J. Optoelectron. Adv. Mater. **8**, 1651 (2006).
[9] V. D. Cojocaru, F. Turquier, R. Nicula, M. Stir, E. Burkel, J. Optoelectron. Adv. Mater. **12**, 397 (2010).
[10] D. L. Decker, J. Appl. Phys. **36**, 157 (1965).

---

*Corresponding author: dan.cojocaru@mdef.pub.ro